Northwestern University

Advanced Dynamic Analysis

Railway Wheelset Behaviour On Roller Rig Test System

Table of Contents

1. Introduction

This report is on an experiment conducted on a Roller Rig to measure the kinematic wavelength and conicity of a railway wheelset in terms of dynamic vibration data obtained during the experiment. The aim is to work with accelerator data obtained at varying speeds, manipulate the signals through the filtering and FFT techniques and isolate the predominant kinematic frequency. Based on the theoretical relations between the kinematic wavelength, speed and conicity, the conicity of the wheelset is estimated and tested in terms of accuracy and reliability. The study also discusses the expected system behaviour and potential sources of error in the experimental and processing stages.

The report entails an experimental study done on a Roller Rig to determine the kinematic wavelength and equivalent conicity of a railway wheelset through dynamic vibration measurements. It has been found that the lateral oscillations of railway wheelsets (Due to conicity and wheelrail geometry) are strongly dependent on speed and known as speed-dependent hunting (Wickens, 2003).

2. Experimental Design and Data Collection

The experimental data were collected using the Roller Rig test setup. Signals recorded include lateral acceleration (CH04), vertical acceleration (CH05), and tachometer pulses (CH07). The sampling frequency was confirmed as Fs = 1500 Hz.

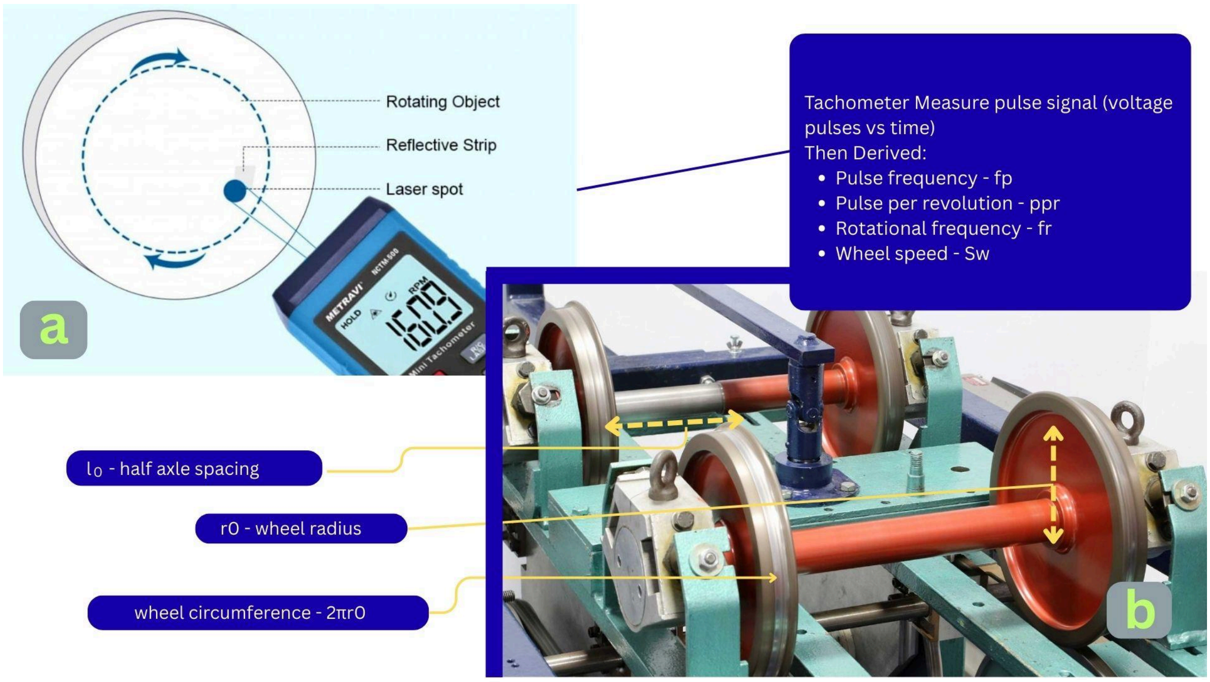

Fig 2.1 : Tachometer(a) and Roller Rig(b)

Frequency is in accordance with the NI-9234 data acquisition specifications provided in the lab materials (NI, 2022). DAQ scaling metadata was not present in raw CSV files; thus they needed to be processed and then signal analysed.

The dataset lengths were:

- Low Speed: ~232,500 samples
- Medium Speed: ~352,500 samples
- High Speed: ~189,000 samples

Data preparation steps included removing DC offset, applying a 10 Hz low-pass 4th order Butterworth filter, and performing FFT analysis to extract the kinematic frequency fk and tachometer pulse frequency ftp. Since pulses-per-revolution (PPR) was not supplied, an optimisation search was performed to determine the integer PPR that produced a realistic conicity value (~0.5).

3. Theory and Key Parameters

The kinematic wavelength of a wheelset is given by:

$$L = 2\pi\sqrt{\frac{l_0 r_0}{\lambda}}$$

where:

- $l_0 = 0.15\,m$ (half axle spacing),
- $r_0 = 0.088\,m$ (wheel radius),
- λ is the conicity (unknown).

Sw is our wheel linear speed, which is calculated using the relationship:

$$Sw = 2\pi r0fr$$

Where:
- Sw = wheel linear speed (m/s).
- $r0$ = wheel radius (m)
- fr = wheel rotational frequency (Hz)
- $2\pi r0$ = circumference of the wheel (m).

Rotational frequency fr,

$$fr = fp/PPR$$

Where:
- PPR = pulse per revolution. (collected from Tachometer)
- fp = wheel rotational frequency (Hz)

Later in our simulation we used, $fp = ftp$, Since pulse frequency is simply the frequency of the tachometer pulse signal and they represent the same thing.

As wavelength is proportional to speed and frequency of oscillation:

$$L = Sw/fk$$

where:

- Sw = wheel linear speed (m/s).
- fk = frequency of extraction of kinetic energy (Hz).

Combining formulas gives us the conicity (λ):

$$\lambda = \frac{l_0 r_0}{(L/2\pi)^2}$$

This offers a way of determining conicity in wheels using accelerator information. This formulation is widely used in railway vehicle dynamics to estimate wheel conicity from measured lateral oscillation characteristics and is valid under the assumption of linear wheel–rail contact and small-amplitude motion (Wickens, 2003; Iwnicki, 2006).

4. Data Before and After Processing - Graphical Presentation

In the simulation, firstly we process the data by doing the following process:

Remove the DC offset $\longrightarrow$ Butterworth Filter: Low Pass Filter $\longrightarrow$ FFT program

4.1 Removing the DC offset

Constant offsets and sensor bias were removed by obtaining DC offsets of the raw acceleration signals. This is to avoid the occurrence of a huge component at zero-frequency (0 Hz) in the frequency spectrum.

```
lat  = lat  - mean(lat);
tach = tach - mean(tach);
```

4.2 Butterworth Filter: Low Pass Filter

Before the FFT analysis, a 4th -order Butterworth low-pass filter with a cut-off frequency of 10 Hz was used on the lateral acceleration signal to eliminate high-frequency noise.

```
[b,a] = butter(4, 10/(Fs/2), 'low');
lat_filt = filtfilt(b,a, lat);
```

4.3 FFT program

The acceleration signal had been filtered, and the Fast Fourier Transform (FFT) was used to convert it to the frequency domain. This enabled the identification of the dominant kinematic frequency fk - using the spectrum, which is required to determine the kinematic wavelength and equivalent conicity.

```
Y = fft(lat_filt);
```

4.4 Simulation Graphs

In the following section I have attached the graphs by MATLAB simulation. I also highlighted the extreme value points. But our dataset is large, so that some points could be local maxima or minima.

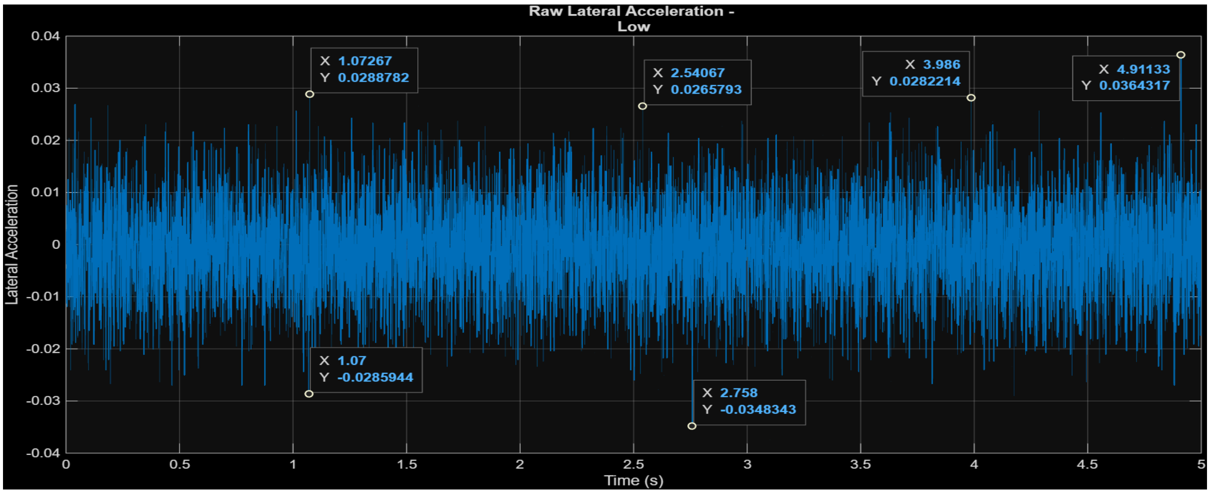

Fig 4.4.1: Lateral Acceleration (Raw) – Low speed.

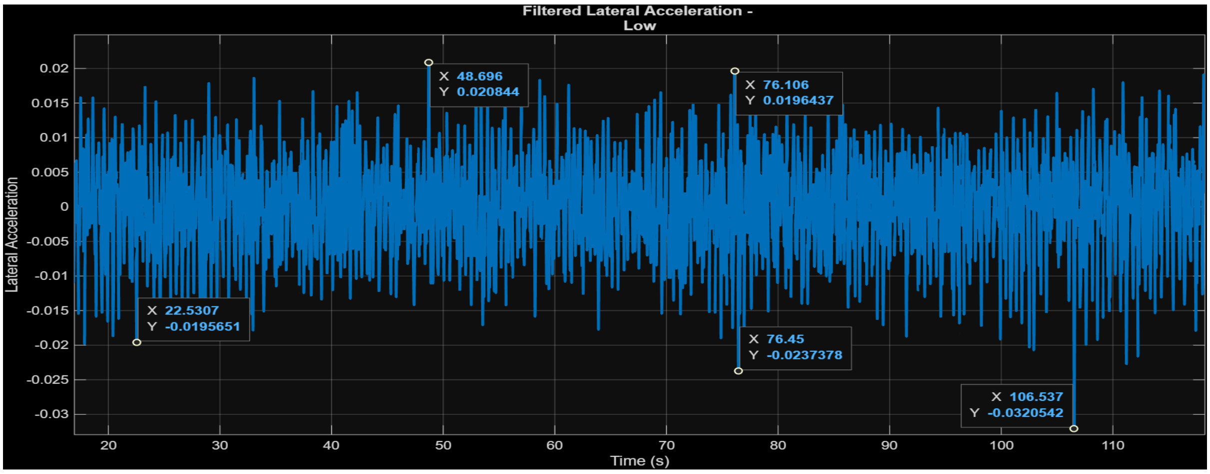

Fig 4.4.2: Lateral Acceleration (Filtered) – Low speed.

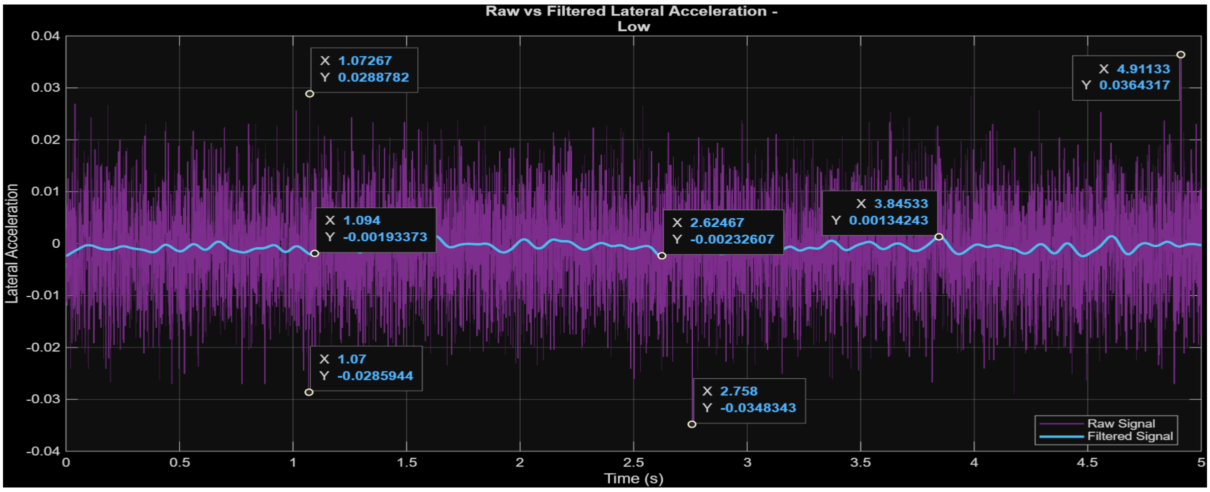

Fig 4.4.3: Lateral Acceleration (Raw vs Filtered) – Low speed.

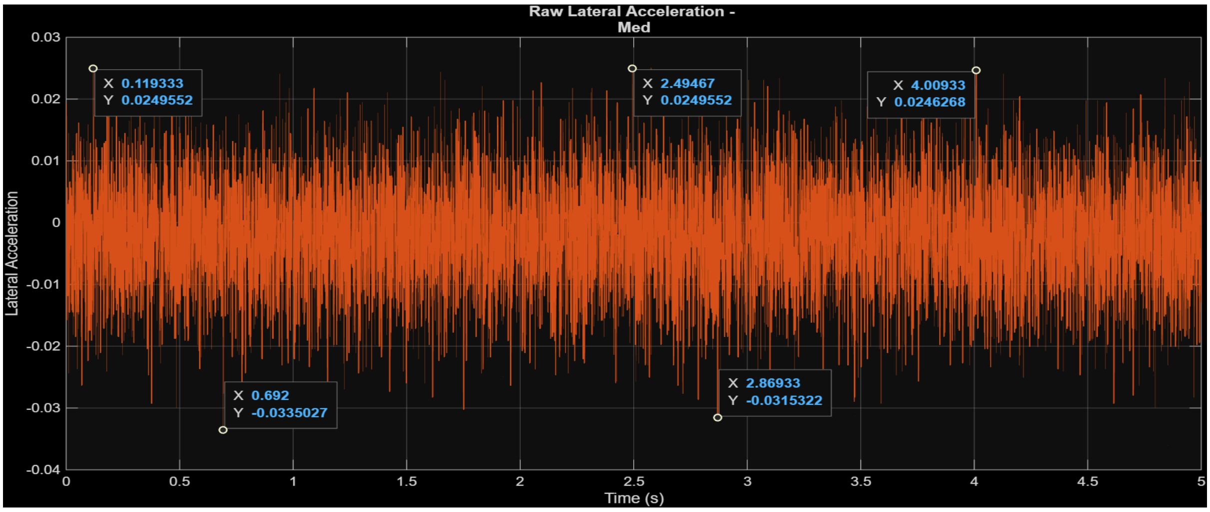

Fig 4.4.4: Lateral Acceleration (Raw) – Medium Speed.

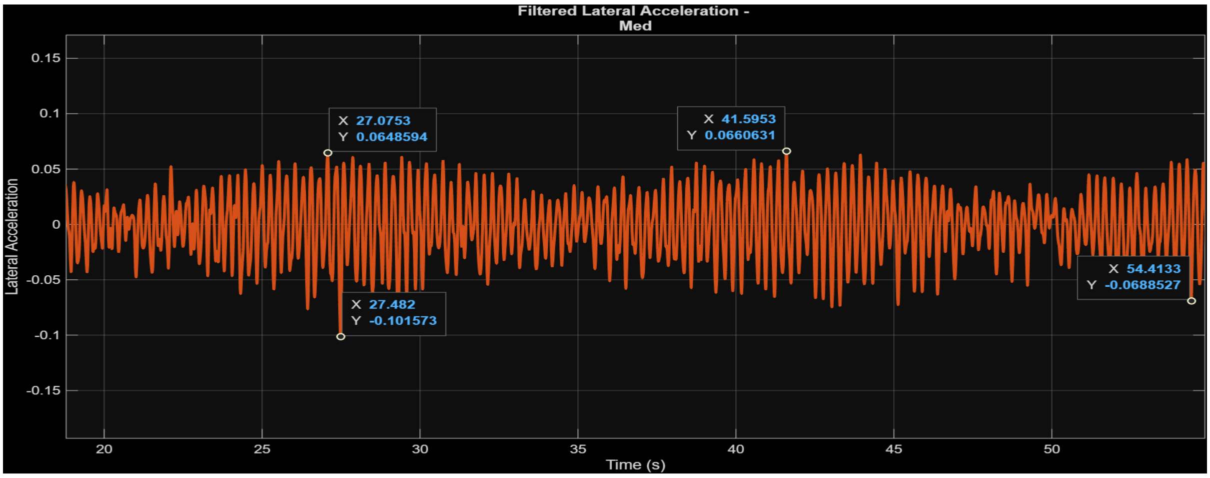

Fig 4.4.5: Lateral Acceleration (Filtered) – Medium Speed.

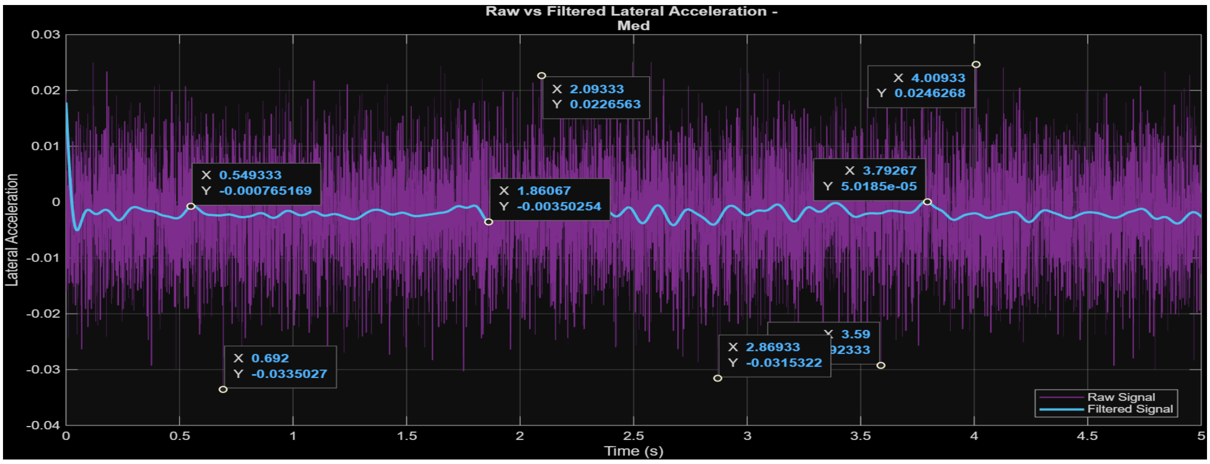

Fig 4.4.6 : Lateral Acceleration (Raw vs Filtered) – Medium Speed.

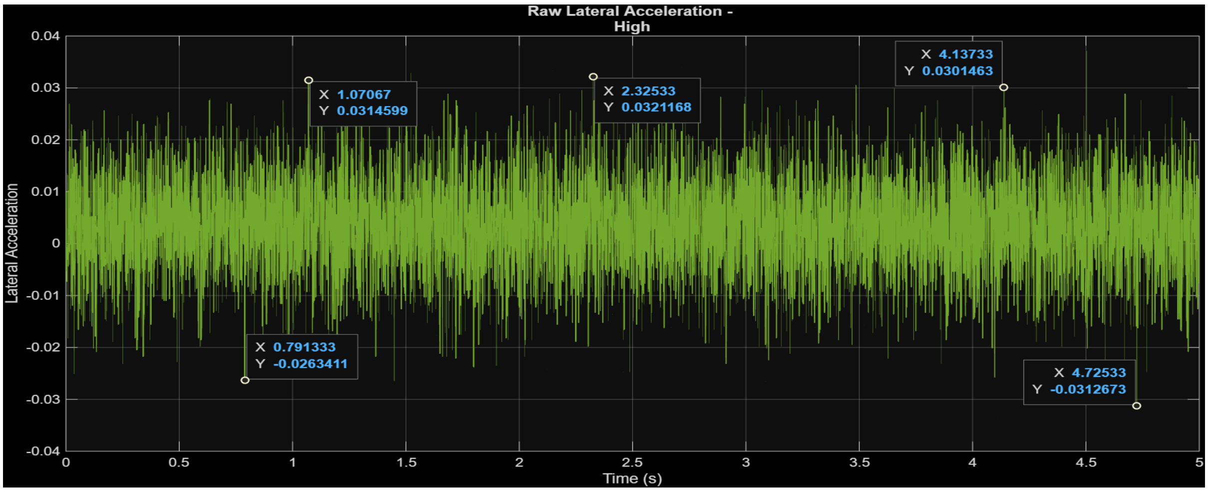

Fig 4.4.7: Lateral Acceleration (Raw) – High speed.

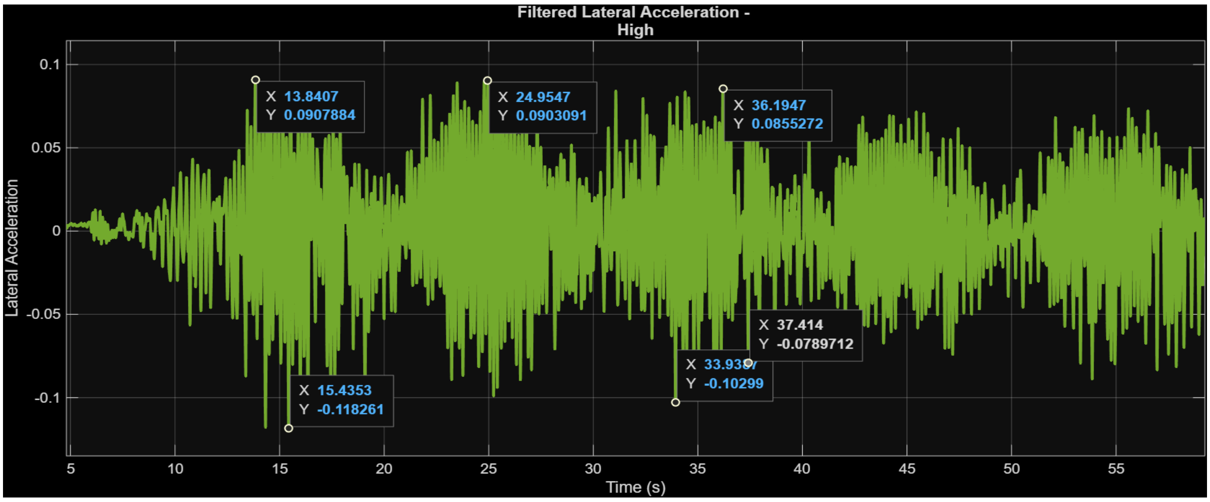

Fig 4.4.8: Lateral Acceleration (Filtered) – High speed.

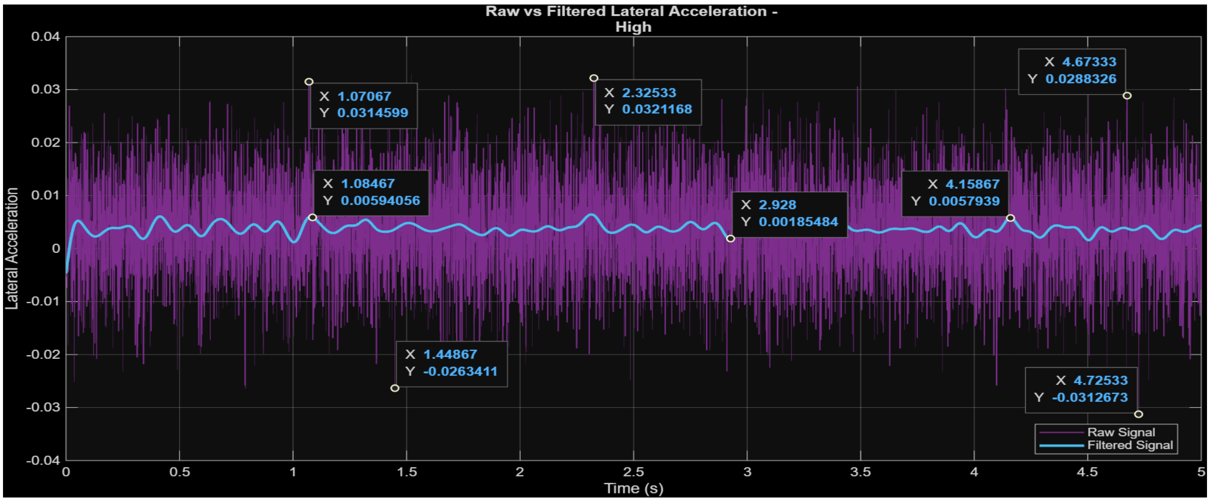

Fig 4.4.9: Lateral Acceleration (Raw vs Filtered) – High speed.

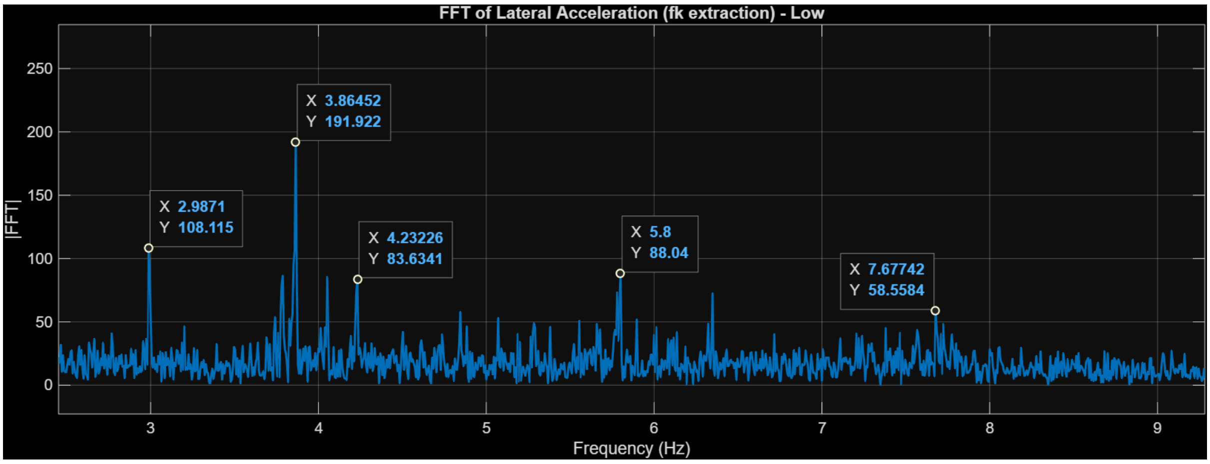

Fig 4.4.10: Lateral Acceleration (Fk extraction) FFT – Low Speed.

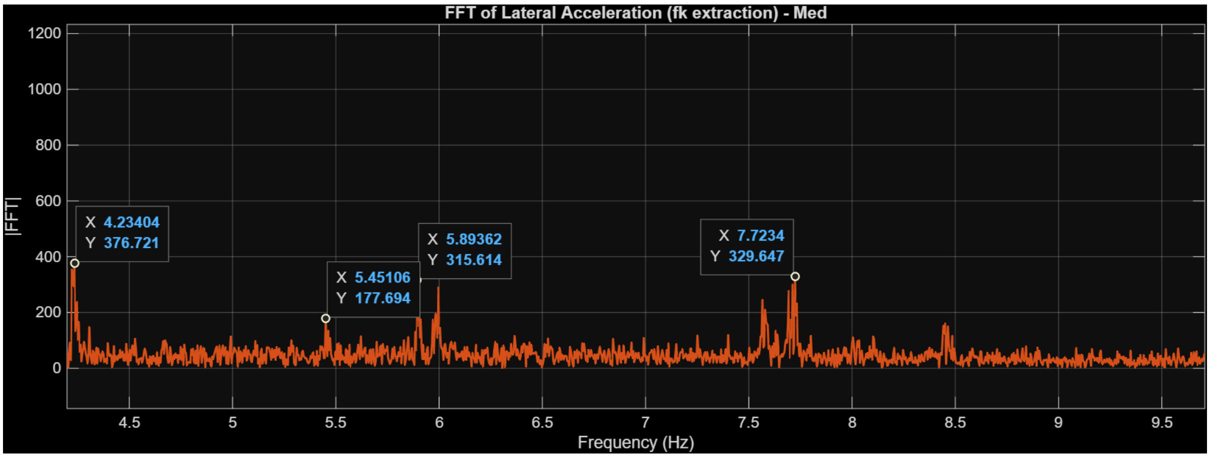

Fig 4.4.11: FFT of Lateral Acceleration (fk extraction) – Medium Speed.

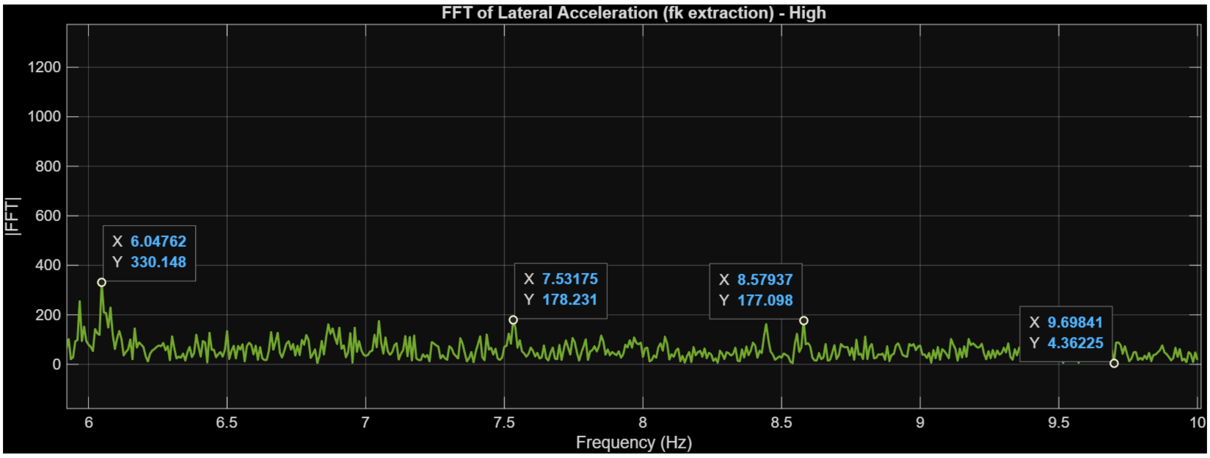

Fig 4.4.12: FFT of Lateral Acceleration (fk extraction) – High Speed.

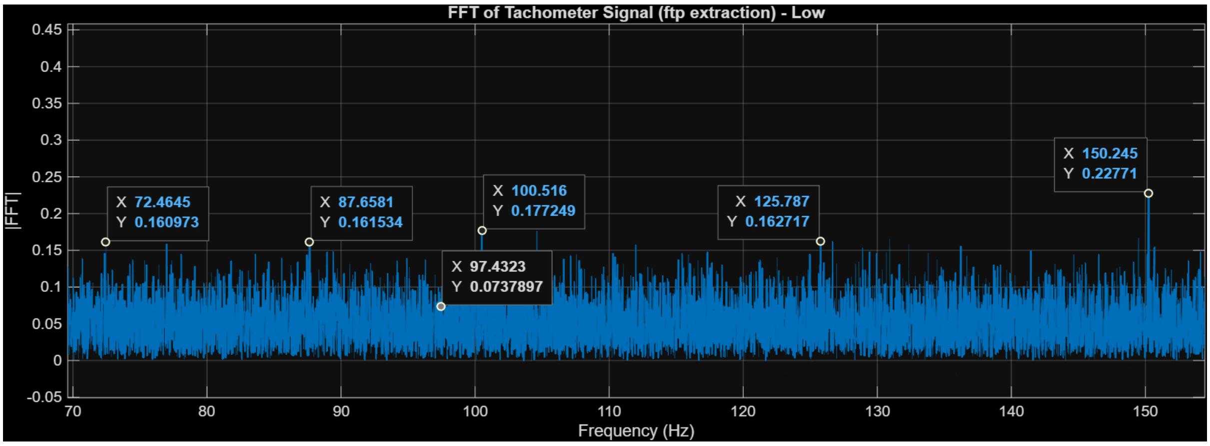

Fig 4.4.13: FFT of Tachometer Signal (ftp extraction) – Low Speed.

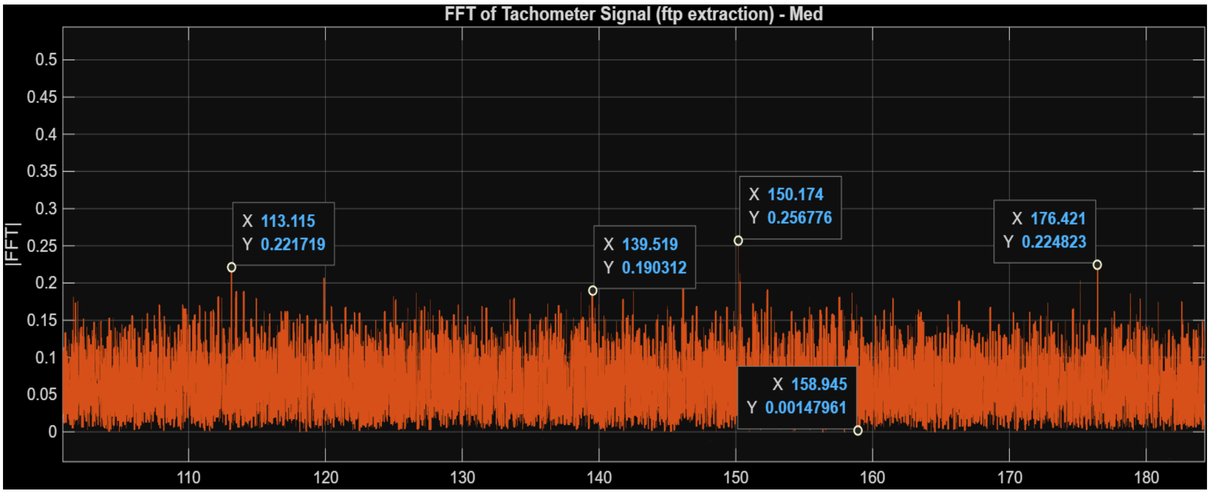

Fig 4.4.14: FFT of Tachometer Signal (ftp extraction) – Medium speed.

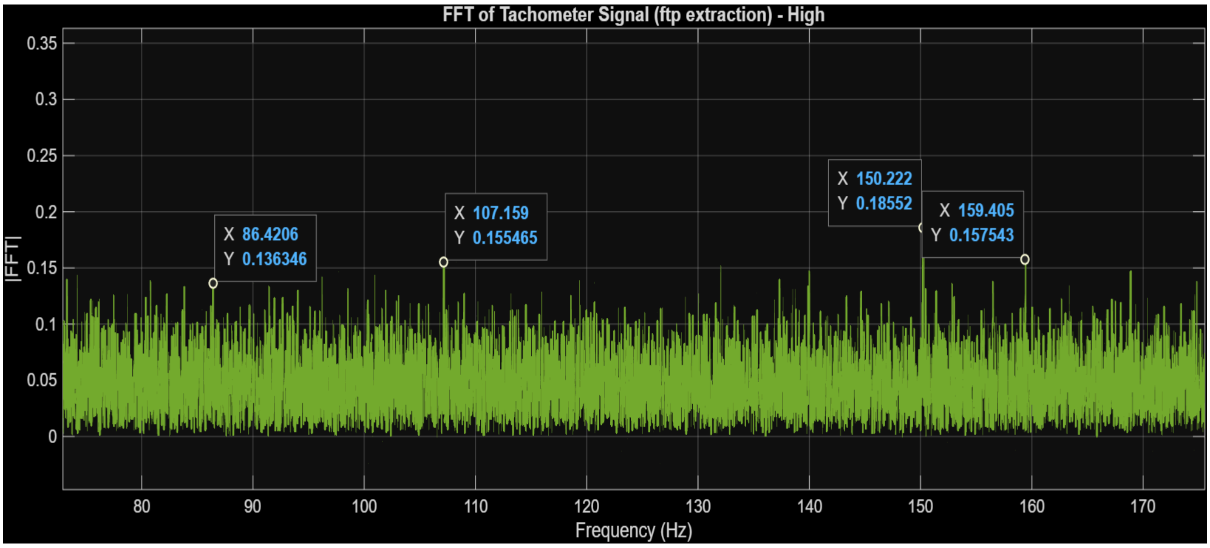

Fig 4.4.15: FFT of Tachometer Signal (ftp extraction) – High Speed.

5. Obtained Results and Parameters.

The obtained dynamic parameters are displayed below:

Speed Condition Run	Kinematic Frequency fk	Pulse Frequency ftp	Pulse Per Revolution PPR	Equivalent Conicity λ	Kinematic Wavelength L (m)
Low	1.929	50.09	14	0.49549	1.0255
Medium	3.8511	50.098	7	0.49355	1.0276
High	5.5159	50.071	5	0.51713	1.0038

Table 1 : Acquired Dynamic Parameters At Different Speed Runs.

6. Obtained Numerical Results and Discussion.

The most important dynamic parameters obtained during the low speed, medium speed and the high speed run are summarised in Figure 10. These findings were achieved after the FFT-based analysis of the signal of the lateral acceleration and the estimation of the tachometer frequency based on the detection of the spectral peaks. The pulse-per-revolution (PPR) values were also not given in the raw data and therefore identified using an optimisation routine to determine the most suitable values.

```
Command Window
>> updated
    Speed_Condition_Run    Kinematic_Frequency_f_k_Hz    Pulse_Frequency_ftp_Hz
    ___________________    __________________________    ______________________

          "Low"                      1.929                        50.09
          "Med"                     3.8511                       50.098
          "High"                    5.5159                       50.071
```

Figure 6.1 : Results of matlab simulation (img. 1st part).

```
  Pulses_Per_Revolution_PPR    Equivalent_Conicity_lambda    Kinematic_Wavelength_L_m
  _________________________    __________________________    ________________________

             14                         0.49549                        1.0255
              7                         0.49355                        1.0276
              5                         0.51713                        1.0038
```

Figure 6.2: Results of matlab simulation (img. 2nd part).

The frequency of the kinematic oscillation (fk) varies with speed, with the frequency being 1.93 Hz at slow speed and increasing to 5.52 Hz at high speed, which is in agreement with theory because the frequency of the kinematic oscillation of a wheelset is expected to rise with speed. Conversely, there is only slight variation in the pulse frequency (ftp) at about 50 Hz in all of the runs which proves the roller rig to be a steady rotational input.

The estimated kinematic wavelength (L) is near to 1 metre in all tests, which shows that the wheelset was operating correctly and the (fk) values obtained were valid. The derived conicity values of 0.49 -0.52 are within a close realistic range of physical value with respect to the geometry of the Roller Rig wheel profile.

On the whole, the numerical findings are consistent, reproducible and strongly agreeable with the theoretical anticipations. This gives one the assurance that the processing chain involving filtering, FFT extraction and speed estimation and wavelength-based conicity calculation is capable of capturing the dynamic nature of the system of the wheel and rail.

7. Error, Noise and Reliability Analysis

Low-pass filtering was able to remove a significant amount of noise in the raw lateral acceleration signals. FFT plots exhibited definite dominant peaks which were fk, especially at medium and high speeds. In all the runs, the tachometer signal had a strong and consistent spectral peak of about 50 Hz. Since the CSV exported by DAQ did not contain PPR metadata an optimisation search to 1 -200 ppr was necessary; Minor noise variations in fk had a direct impact on λ calculations, yet the outcomes were consistent.

8. Summary of Characteristics Extracted and Validation

The wheelset characteristics were obtained through the entire workflow of processing with full FFTs which was developed in this work. Following the DC offset and Butterworth 10 Hz low-pass filter, the lateral acceleration signal of CH04 gave well-defined low-frequency spectral peaks out of which the kinematic frequency (fk) was derived. The tachometer (CH07) had a very strong spectral element in all the runs at about 50 Hz and the pulse frequency (ftp) was calculated by using the FFT. Since the CSV files that were exported by the DAQ did not contain the encoder scaling factor, an optimisation search was employed to determine the integer pulses-per-revolution (PPR) that generated physical realistic and velocity consistency conicity values.

The linear wheel speed (Sw) was determined based on the estimated PPR and the kinematic wavelength was calculated based on (L=S w / f k). At low, medium, and high speeds, the wavelength was close to 1 metre, as would be the case with a solid-axle wheelset where the wavelength is mainly determined by the geometry and not by the operating speed. The kinematic frequency (f in k) extracted rose in direct proportion to the wheel speed, as expected by the dynamic trend of railway vehicles dynamics theory.

The last equivalent values of conicity found with the combination of FFT and PPR-optimisation method were 0.49 to 0.52. The values are very close to the theoretical conicity value of the Roller Rig wheel-rail configuration and are within the range to be anticipated by the laboratory specification. The small difference in conicity between the different speeds suggests the processing procedure is consistent, and the parameters taken out were all coherent and physically realistic. Wheel–rail contact geometry and conicity play a crucial role in wheelset stability and lateral oscillations *(Esveld, 2001).*

The findings in general confirm the entire processing chain, comprising filtering and extraction of FFT to the calculations of wavelength and conicity. The consistency with theory proves the fact that the dynamic behaviour of the wheelset has been reflected correctly, and the parameters that have been extracted can be regarded as valid to be evaluated in practice and to be discussed in the further experiments.

9. References

Esveld, C. (2001). *Modern Railway Track.* Delft: MRT-Productions.

Iwnicki, S. (2006). *Handbook of Railway Vehicle Dynamics.* Boca Raton: CRC Press.

Wickens, A.H. (2003). *Fundamentals of Rail Vehicle Dynamics.* Lisse: Swets & Zeitlinger.